Available online at www.sciencedirect.com
SCIENCE DIRECT®
Polymer 45 (2004) 3377–3387
polymer
www.elsevier.com/locate/polymer

Degradable networks formed from multi-functional poly(vinyl alcohol) macromers: comparison of results from a generalized bulk-degradation model for polymer networks and experimental data

Penny J. Martens[a,1], Christopher N. Bowman[a], Kristi S. Anseth[a,b,*]

[a]Department of Chemical and Biological Engineering, University of Colorado, Campus Box 424, Boulder, CO 80309, USA
[b]Howard Hughes Medical Institute, University of Colorado, Boulder, CO 80309, USA

Received 8 December 2003; received in revised form 1 March 2004; accepted 4 March 2004

Abstract

Experimental and theoretical approaches were used to understand the degradation behavior of networks formed from the chain polymerization of multi-functional macromers. A typical experimental mass loss profile and theoretical model are presented and discussed to illustrate the various regions of erosion. Specifically, the degree of connectivity of the network was shown to influence the percent mass loss at reverse gelation, and the percent cyclization was shown to influence the overall shape of the mass loss profile. Finally, the theoretical predictions of mass loss were compared to experimental data for macromers with variations in their molecular weight and degree of functionality (i.e. variations in the initial network crosslinking density). Changes in the volumetric swelling ratio and compressive modulus were measured with time to obtain the degradation kinetic constant for each macromer system, ranging from $1.5 \times 10^{-4}\,\mathrm{min}^{-1}$ to $3.0 \times 10^{-5}\,\mathrm{min}^{-1}$. Results demonstrate that the theoretical predictions capture the mass loss profiles of all three systems, and as the crosslinking density of the initial network was decreased the overall time for complete degradation of the gels was also decreased.

Keywords: Degradable polymers; Hydrogels; Computer modeling

1. Introduction

In recent years, an emerging area of interest in the biomaterial field is in situ forming crosslinked networks, particularly degradable networks formed from multi-functional macromers [1–7]. Several groups [3,5,7–16] have designed new multi-functional macromer chemistries that systematically incorporate degradable units into networks; however, the degradation behavior and mass loss profile of these materials can be quite complex. Thus, to better characterize these systems, theoretical models that address the complexity that is brought about by structural features and the degradation mechanism in crosslinked networks are beneficial. Specifically, crosslinking leads to an increase in the number of structural configurations that can exist, and these configurations change throughout the degradation process. Additionally, unlike linear systems where bond scission and molecular weight are directly related, these relationships do not necessarily hold true for crosslinked polymer structures. For example, in linear degradable systems if a bond is cleaved (i.e. degraded) and the resulting polymer segment is small enough, it becomes soluble in the surrounding media and produces a loss in the mass of the sample (i.e. erosion). However, in crosslinked networks degradation and erosion are strongly dependent on the connectivity and structure of the network, which often requires the degradation of multiple links to the network before erosion occurs.

In our first attempt to better understand and predict the degradation behavior of crosslinked networks, a theoretical model was developed to describe the bulk-degradation behavior of hydrogels formed from divinyl macromers (e.g. PEG based diacrylate macromers) [17,18]. In this work, Metters et al. [17] presented an approach to account for both structural and kinetic parameters of hydrogels with degradable blocks in the crosslinks. For example, the mass loss of

* Corresponding author. Tel.: +1-303-492-3147; fax: +1-303-735-0095.
E-mail address: kristi.anseth@colorado.edu (K.S. Anseth).
[1] Current Address: University of New South Wales, Graduate School of Biomedical Engineering, Sydney, New South Wales 2052, Australia.

0032-3861/$ - see front matter © 2004 Elsevier Ltd. All rights reserved.
doi:10.1016/j.polymer.2004.03.011

the hydrogels was predicted as a function of degradation time for many different parameters, including the number of crosslinks in the kinetic chain and the hydrolysis rate constant. Numerous non-idealities associated with the network structure and variations in the degradation kinetics (i.e. incomplete conversion of the double bonds or incomplete functionalization during the synthesis of the macromer) were subsequently incorporated into the model [18]. These non-idealities allowed for the successful prediction of temporal changes in swelling [19,20], compressive modulus [19,20], mass loss [17–20], and drug release [20] as a function of degradation. These non-idealities resulted in either shorter degradation time predictions or an increased mass loss at early degradation times, depending on how the partially reacted chains were incorporated into the network [18].

Based on the insight gained from modeling degradable networks formed from divinyl monomers, we sought to develop a more general model, capable of predicting the degradation behavior of hydrogels formed from any *multi-vinyl* crosslinking molecule with degradable segments located in the crosslinks [21]. The structure and degradation behavior of hydrogels formed from multi-vinyl macromers are likely to be very different from that seen for the PEG based gels; however, the same statistical-kinetic approach to predicting their behavior is applicable. Briefly, the main difference between the PEG-based model and this more generalized model is the number of possible structural configuration that exist in the multi-vinyl systems. The generalized model uses a statistical approach to predict and track the different configurations of the crosslinking molecules and kinetic chains, and kinetic information to ascertain the probability that a degradable linkage is intact. The statistical and kinetic portions of the model are then combined to determine whether the polymer segments are releasable. The development of this generalized model is presented in detail elsewhere [21], but it has yet to be validated through an experimental system that enables systematic variations in the network chemistry and structure.

To this extent, degradable, multi-functional poly(vinyl alcohol) (PVA) macromolecular monomers were synthesized and characterized experimentally to provide a system to verify the model predictions. This system was developed to verify the results of the model because it captures several key features. First, the model assumes that the networks degrade homogenously; therefore, the gels must have high water content. Since PVA is hydrophilic, all of the macromers studied form hydrogel networks with high water content (>90% water). Another benefit of these macromers is that the number of functional groups on the macromer can be changed by either changing the molecular weight of the original PVA chains or by varying the amount of pendent alcohol groups that are modified with the crosslinkable groups. In addition, the final network structure can be varied by slightly modifying the polymerization conditions. These simple, yet diverse, methods provide an easy way to systematically vary the final network structure, which is important when attempting to validate a model.

Specifically, in this work, characterization and validation of a model developed to predict mass loss from hydrogels formed from multi-vinyl macromer chain polymerizations were undertaken. A typical experimental mass loss profile is shown to describe the three main regions of mass loss. To further understand how the various network properties influence the different regions of mass loss, structural aspects of the network, including the kinetic chain length and connectivity, as well as the network cyclization, were varied in the model to obtain a range of mass loss profiles. Next, the model predictions were validated with experimental systems based on multi-functional, degradable PVA macromers. The volumetric swelling ratio and compressive modulus were measured as a function of time for all of the experimental systems. The hydrolysis rate constant was calculated from the experimental volumetric swelling and compressive modulus data and was used in conjunction with the model to predict mass loss profiles for the experimental systems. The experimental and theoretical mass loss profiles are shown and compared for three PVA networks with a range of crosslinking densities.

2. Materials and methods

2.1. Multi-vinyl PVA macromer synthesis

Poly(vinyl alcohol) (PVA, Clariant) was modified with degradable, crosslinkable pendant groups, as described elsewhere [22,23]. Briefly, mono-2-(acryloyloxy)ethyl succinate (AOES, Aldrich) was extended with succinic anhydride to produce a 5-ester acrylate molecule, which was then attached to the PVA via the pendant hydroxyl groups (see Fig. 1). The 5-ester acrylate molecules were coupled to the PVA (Acr-Est-PVA), and the presence of resonances for the vinyl protons ($\delta = 6.4$ ppm, d, $\delta = 6.1$ ppm, q, $\delta = 5.8$ ppm, d) was seen in ^{1}H NMR. The spectra were collected in D_2O.

To quantify the average number of pendant ester-acrylate groups on the PVA, the polymerization of the Acr-Est-PVA was monitored using differential scanning calorimetry (DSC) (Perkin–Elmer DSC-7). Because of the low concentration of vinyl groups, we were unable to use ^{1}H NMR to quantify the percent acrylation accurately; however, DSC provides a quick and relatively sensitive means to characterize this parameter. The DSC head was modified with quartz windows to allow for the transmission of initiating light, and a high intensity light source equipped with a 365 nm band-pass filter was used to initiate the polymerization at an intensity of ~ 20 mW/cm^2. The polymerizations were carried out in air at 25 °C. To prevent evaporation, plastic lids were placed over the samples in the DSC pans prior to polymerizing. Since the polymerization

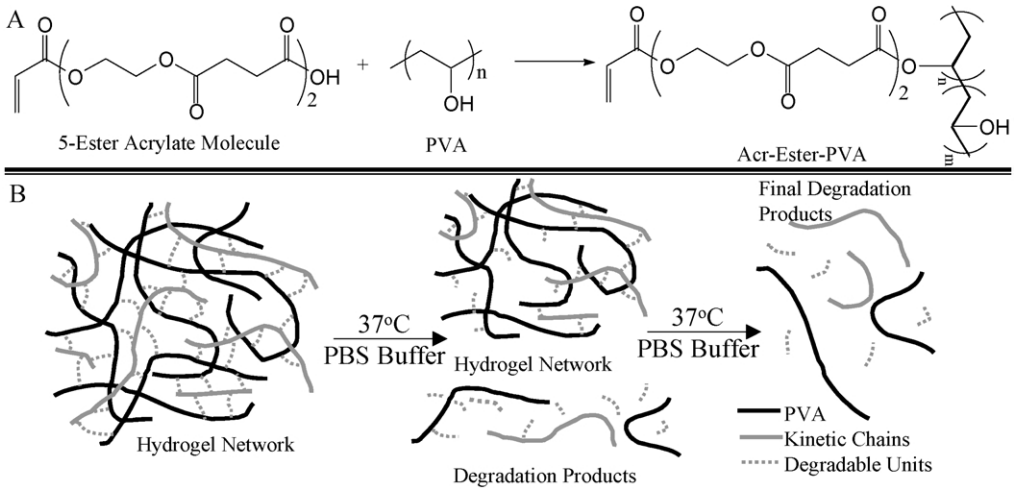

Fig. 1. (A) Schematic of the attachment of the 5-ester acrylate molecule to the PVA chains and the subsequent macromer that is formed. (B) Schematic of the hydrogel networks and the subsequent degradation process and products.

of the Acr-Est-PVA macromer solution is an exothermic reaction, the heat released by the sample is related to the rate of polymerization by the following equation:

$$R_P = \frac{Q}{\Delta H_{theor} \text{wt frac} m} \quad (1)$$

where R_P is the rate of polymerization (s^{-1}); Q is the heat flow (kcal/s); ΔH_{theor} is the heat of reaction for the acrylate functionality (kcal/mol); and wt frac is the sample mass divided by the total mass of the macromer chain (g/g). The final parameter in the rate equation is m, which is the moles of acrylate per PVA chain (mol), or simply the average number of pendant vinyl groups per PVA chain. Furthermore, the conversion, X, can be calculated by integrating the rate profile.

$$X(t) = \int_0^t R_p dt \quad (2)$$

Then, if one assumes complete conversion of the acrylate groups (based on Near-IR experimental results presented in Martens and Anseth [24]), m can be calculated if ΔH_{theor} is known.

$$m = \frac{1}{\Delta H_{theor} \text{wt frac}} \int_0^t Q \, dt \quad (3)$$

The ΔH_{theor} was determined by polymerizing a small sample of AOES in the DSC. AOES was chosen because of its structural similarity to the acrylate functionality on the PVA, and since it is monovinyl it is easy to analyze. We expected complete or near complete conversion upon polymerization of this linear system, and no vinyl signal was detectable by FT-IR (>95% conversion). From these experiments, ΔH_{theor} for these acrylates was then calculated as 16.5 ± 0.8 kcal/mol. This value is somewhat lower than the 20.6 kcal/mol that is often cited for lower molecular weight multi-functional acrylates [25], but within the range of values that are reported for acrylates in the literature. Several different macromer compositions were synthesized and characterized in this work, and their compositions are given in Table 1.

2.2. Gel preparation

The Acr-Est-PVA macromers were dissolved in DI-H_2O at 80 °C to a final concentration of 20 wt%. The photoinitiator, 2-hydroxy-1-[4-(hydroxyethoxy) phenol]-2-methyl-1-propanone, (Irgacure 2959, I2959, Ciba-Geigy) was used as supplied and dissolved in DI-H_2O to a final concentration of 0.05 wt% in all formulations. The macromer/initiator solution was photopolymerized under cytocompatible conditions using an ultraviolet light source (Novacure, EFOS, Inc.) at an intensity of 5–20 mW/cm^2 for ≤10 min [26].

Immediately after polymerization, the sol fraction was extracted from the gel by soaking the gels in water for 24 h. The sol fraction was approximately 40 wt% in each of the gels and was further characterized using ^{1}H NMR, gel permeation chromatography (GPC), and by titration of the carbon–carbon double bonds. Combining the results from the characterization techniques [27], the high sol fraction was attributed to either unmodified PVA chains or PVA chains with a very low percent modification and not reacted into the network.

2.3. Characterization of gel properties

Volumetric swelling, compressive modulus, and mass loss were measured throughout the degradation of the poly(Acr-Est-PVA) networks. Degradation of the polymerized hydrogels was carried out in PBS at 37 °C. Disks (10 mm in diameter and 1 mm thick) were polymerized in molds, weighed immediately following polymerization, placed in a permeable, plastic tissue cassette, and degraded in buffer solution under sink conditions. At various time

Table 1
Compositions of the Acr-Est-PVA macromers

Initial PVA molecular weight (g/mol)[a]	Number of pendant vinyl groups[b]	Percent of network mass contained in: PVA/degradable units/kinetic chains (wt%:wt%:wt%)
16,000	5	89.9/6.9/3.2
14,000	3	92.8/4.9/2.3
31,000	2	97.7/1.5/0.8

[a] As supplied by the manufacturer.
[b] As measured by DSC.

points, a tissue cassette was removed from the buffer solution, patted dry, and weighed to obtain the swollen wet weight of the disk (m_s). The disk was then thoroughly dried by lyophilization, and a final dry weight was obtained (m_{fd}). The initial dry polymer mass (m_{id}) was calculated by multiplying the initial wet weight of the disk by the weight fraction of macromer in solution during network formation. The percent mass loss from each sample was determined using the following equation:

$$\%\ \text{mass loss} = \frac{(m_{id} - m_{fd})}{m_{id}} 100\% \tag{4}$$

Note that the mass loss reported in all figures first corrects for the initial mass loss due to the soluble fraction. Therefore, the data reported is only related to the mass loss due to network degradation.

The volumetric swelling ratio (Q) was calculated via the mass swelling ratio ($q = m_s/m_{fd}$) according to the following equation:

$$Q = 1 + \frac{\rho_{polymer}}{\rho_{solvent}}(q - 1) \tag{5}$$

Here, $\rho_{polymer}$ is the macromer density and was approximated by the density of PVA ($\rho_{PVA} = 1.2619$ g/ml). $\rho_{solvent}$ is the density of the buffer solution and was approximated as 1.0 g/ml.

In addition, the compressive modulus was characterized as a function of degradation time. Polymer disks (initial diameter and thickness of 10 and 1 mm, respectively) were swollen in PBS buffer at 37 °C, and samples were removed at various points throughout the degradation process. Disks (3.9 mm diameter, 0.5–2 mm thick) were punched out of the samples, and their static compressive modulus was measured using a dynamic mechanical analyzer (Perkin–Elmer DMA-7) with a parallel plate configuration. The samples were surrounded by water to prevent deswelling during the test and were compressed at a rate of 10 mN/min. The slope of the stress–strain curve in the linear region (~5–15%) was used for the modulus calculations.

2.4. Statistical analysis

In all plots presented in this paper, the error bars represent ± one standard deviation from the average. In addition, the y-axis error bars were calculated from at least three samples taken at the same time point, and x-axis error bars are a result of variation in either the time the sample was taken or the variation in the total time required for degradation (i.e. the final mass loss data point).

2.5. Theoretical model of network degradation

Our chosen modeling scheme was applied to hydrogels formed from the chain polymerization of multi-functional macromers containing degradable crosslinks [21]. The model is a generalized form of a statistical, mean-field approach originally developed for networks formed from divinyl macromers [17,18]. Briefly, degradable blocks within the network are assumed to hydrolyze with pseudo first-order kinetics (k'). This information is combined with structural information about the connectivity of segments in the network to determine the probability that the crosslinks (i.e. PVA chains) or kinetic chains are releasable. Finally, reverse gelation is incorporated by determining the weight average number of crosslinks per kinetic chain [28]. When this number drops below two, the network transitions to a highly branched system that is completely soluble.

For simplification, all of the crosslinking molecules were assumed fully reacted during network formation, implying that all degradable segments exist as either crosslinks or cycles between the kinetic chains. This assumption is a reasonable approximation for these networks, as similar multi-functional PVA macromers have been shown to reach 100% conversion of their double bonds as measured by Near-IR Spectroscopy [24]. Each degradable 'arm' from the multi-vinyl crosslinking molecule was considered as a single, degradable block, which captures the fact that when one of the ester bonds is broken the entire crosslink is broken.

All of the experimentally modeled networks are highly swollen ($Q > 10$), and therefore, the hydrolysis of the degradable units was assumed to occur homogeneously following pseudo first-order kinetics. Also, due to the highly swollen nature of these networks, the diffusion of degradation products out of the crosslinked systems was assumed to occur much more rapidly than hydrolysis. Thus, once all of the linkages connecting a certain chain to the network are broken (i.e. degraded), the chain is considered to be released (i.e. eroded from the network) and no longer contributes to the network mass. While fast release is expected, mass transport of the releasable segments could be added to the model. To date, this general model predicts degradation for networks where there are more crosslinking molecules per kinetic chain, n, than there are vinyl groups on the crosslinking molecule, m, due to the specific way in which the model equations were written. However, the case when

$m > n$ can be easily simulated by simply reversing the annotations in the code. For simplicity, the additional assumption of monodisperse chain lengths within the gels is assumed, and chain transfer reactions during network formation are neglected.

Structural information about the hydrogel is incorporated into the model to relate degradation of the ester blocks to hydrogel erosion. Due to the relatively small fraction of mass residing in the kinetic chains and degradable units (i.e. $<15\%$ compared to the PVA chains), these molecules were lumped together, and the generalized mass loss equation from these gels was written as a function of the two types of molecules that are released:

$$\%\ \text{mass loss} = (W_{xl}F_{xl} + W_{kc}F_{kc}) \quad (6)$$

Here, F_{xl} is the fraction of crosslinking molecules (i.e. PVA chains) that are releasable from the gel, while F_{kc} is the corresponding fraction of kinetic chains and degradable units that are releasable. Similarly, W_{xl} is the mass percent of the original crosslinked network contained in the crosslinking molecules, while W_{kc} is the mass percent in the kinetic chains and ester blocks combined. W_{xl} and W_{kc} are constants that are based on the chemical structure of the starting macromers. Determining the time-dependent erosion profiles of these crosslinked gels, therefore, depends on calculating F_{xl} and F_{kc} as functions of degradation time. Thorough descriptions of each of these parameters are provided in detail in Martens et al. [21].

3. Results and discussion

Before comparing experimental results and theoretical predictions, a typical experimental mass loss profile for a network synthesized from a multi-vinyl PVA macromer is shown in Fig. 2. The mass loss profile shown in Fig. 2 is for a 16,000 g/mol PVA macromer with an average of five pendant vinyl groups per chain. In general, there are three main regions of mass loss, as highlighted in Fig. 2. Region 1 is an initial period of little or no mass loss where degradable bonds are being cleaved, but no erosion is occurring due to the high degree of inter-connectivity present in these gels. Region 2 is a period of relatively steady mass loss where a significant fraction of the degradable segments have been cleaved, and PVA chains are released along with a few kinetic chains. The final region, region 3, is termed reverse gelation and occurs when degradation leads to polymer chains that are no longer connected into an infinite network, but rather are highly branched, soluble chains.

To better understand the various regions of the mass loss profile and to tune the network erosion profile, a statistical-kinetic model was developed [21]. The model has five adjustable parameters: the number of crosslinkable functionalities on the PVA chain (m), the weight percent of the network contained in the crosslinking molecules (i.e. PVA chains, W_{xl}) relative to the kinetic chains ($W_{kc} = 1 - W_{xl}$),

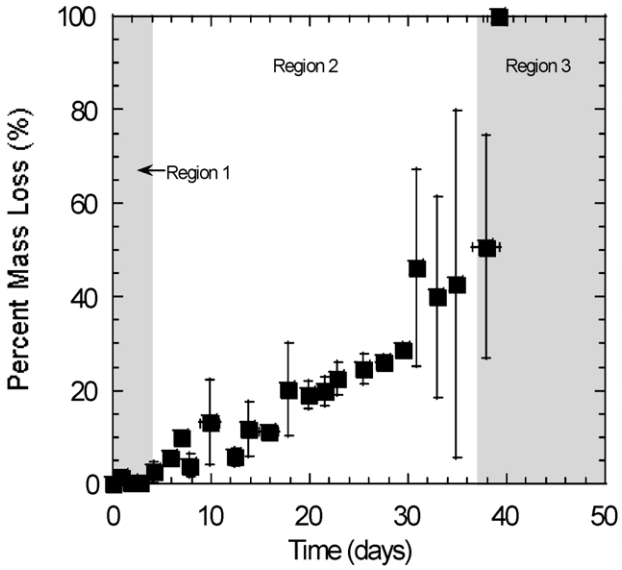

Fig. 2. Typical experimental mass loss profile for a network formed from a 20 wt% solution of the 16,000 g/mol PVA with an average of five pendant vinyl groups per PVA chain. The large error bars at later time points are reflective of the difficulties in sample handling at later stages of degradation. The three main regions of mass loss are highlighted. Region 1 is the initial delay where very little or no mass loss occurs; region 2 is a relatively steady loss of polymer chains; and region 3 is reverse gelation (i.e. the entire network becomes soluble).

the number of crosslinks in the kinetic chain (n), the hydrolysis kinetic constant of the degradable blocks (k'), and the propensity of the double bonds to form crosslinks versus cycles (Ψ_1). While adjustable, each of these parameters is related to a physical aspect of either the original macromer or the resulting network structure and has various effects on the mass loss profile. The first two parameters, m and W_{xl}, are directly related to the initial macromer that is used to form the network and are known once the macromer has been fully characterized. Because of the low percent substitution of the macromers used in this work, the number of crosslinkable functionalities on the PVA, m, was controlled synthetically and confirmed experimentally via DSC. The value of m was determined to within $\pm$ one functional group. W_{xl} was directly calculated from the initial weight ratios in the macromer structure (Table 1). Furthermore, an increase in m lengthens the time it takes to reach region 3 of the mass loss profile, and increasing W_{xl} results in an increase in the total mass that is lost before region 3 [21]. The number of crosslinks in the kinetic chain, n, is related to the kinetic chain length and to the point at which the remaining network becomes completely soluble (i.e. when region 3 occurs). The average kinetic chain length can be controlled by the polymerization conditions. Reverse gelation results in the entire network becoming soluble and occurs when the weight average number of crosslinks per kinetic chain is less than two [28].

$$n_{xl} = n(1 - P)(1 - P^{m-1}) \quad (7)$$

Here, n_{xl} is the average number of crosslinks per kinetic chain at any point throughout degradation, and P is probability that any random degradable block has been hydrolyzed. If $n_{xl} \leq 2$, then there are no more than two crosslinks per kinetic chain and reverse gelation occurs. Therefore, reverse gelation is an indication of how many crosslinks there are in the kinetic chain [21].

The degradation kinetic constant (k') is a measure of how fast the degradable linkages will be cleaved and influences the overall time for mass loss [21]. In this work, k' was calculated from the volumetric swelling data and further verified by the compressive modulus data. It should be noted that k' varies over a wide range of values, but the relative error associated with k' is relatively small (less than $\pm 0.6 \times 10^{-5}\ \mathrm{min}^{-1}$). In this work and in others [17], it has been experimentally observed that the rate of hydrolysis depends not only on the ester chemistry but also on the length of the degradable block and the local network structure. The final parameter, Ψ_1, is a physical measure of how the different chains are connected into the network, and it is the most difficult parameter to measure directly. Ψ_1 is constant for a given system, and can have values between 0 and 1. A Ψ_1 value of 0 indicates that no cyclization is present and a value of 1 means that every pendant functional group has reacted with another functional group on the same PVA backbone, and thus the system is 100% cyclized. Due to the difficulty and large error that would be present in experimentally measuring Ψ_1, it was treated as an adjustable parameter that was fit to the experimental mass loss data. Other investigators have developed fairly elaborate kinetic models that, when combined with experiments of crosslinking polymerizations, can be used to estimate Ψ_1 [29]. In addition, one could use rubber elasticity theory to estimate the deviation of the measured concentration of elastically active chains from an ideal network structure. While not trivial, Ψ_1 could then be inferred from the estimated ratio of the intra- to intermolecular crosslinks. The influence of changing the cyclization parameter on the mass loss profile is explored in greater detail below. In addition, the average number of crosslinks per kinetic chain was calculated throughout the degradation and related to the gel's volumetric swelling ratio and the compressive modulus to provide insight into macroscopic properties. Through the combined degradation kinetics and structural information, the model was used to predict the total network mass loss during degradation, as well as the release of the kinetic chains and the crosslinking molecules, as a function of the model parameters.

Understanding how the five parameters influence the various aspects of the mass loss profiles, either independently or in conjunction with other parameters, provides insight into how these complicated networks are assembled. For example, the percent mass loss at the time of reverse gelation is influenced by the length of the network chains and the ways in which they are connected. In Fig. 3, the functionality of the PVA macromer, m, and the number of crosslinks in the kinetic chain, n, were systematically varied while the other model parameters were held constant and no cyclization was present. The value for the kinetic constant, $k' = 4.5 \times 10^{-5}\ \mathrm{min}^{-1}$, was selected as a mid-range k' value for this type of degradable gel chemistry [23,30]. For a given number of crosslinkable functionalities on the PVA chain (e.g. two vinyl groups, $m = 2$), as the number of crosslinks in the kinetic chain is increased, the percent mass loss at the time of reverse gelation is increased. When there are an equal number of network connections on the PVA and kinetic chains (e.g. $m = 2$ and $n = 2$), a minimum amount of mass loss occurs before reverse gelation. As the ratio between m and n decreases, the number of crosslinks per kinetic chains increases, and therefore, more of the network erodes before reverse gelation occurs. Since the PVA chains are only connected by a small number of crosslinks, when $m/n \ll 1$ they erode from the network first compared to the more highly connected kinetic chains. As the kinetic chains get longer ($m/n \rightarrow 0$), the percent mass loss at reverse gelation approaches the weight fraction of PVA in the system. The same principles can be applied when increasing the number of crosslinkable functionalities on the PVA, m, for a fixed n. As the PVA is further connected into the network, a higher percent mass loss occurs before reverse gelation.

Another interesting set of model parameters to examine is how cyclization (Ψ_1) and the number of crosslinks per kinetic chain (n), and especially their synergistic effects, influence the shape of the mass loss profile. By changing these two parameters, either separately or together, significantly different profiles result. For the examples

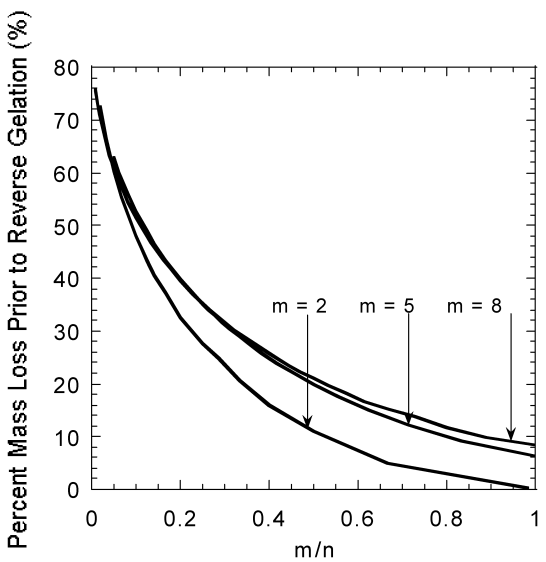

Fig. 3. Percent mass loss at reverse gelation as a function of the ratio between number of vinyl groups on the PVA chain, m, and the number of crosslinks in the kinetic chains, n. The three curves show an increase in the number of crosslinkable functionalities on the PVA chains, and therefore, a decreasing W_{xl} ($W_{xl} = 0.957$, 0.899 and 0.847 for $m = 2$, 5, and 8, respectively) Other model parameters were: no cyclization and $k' = 4.5 \times 10^{-5}\ \mathrm{min}^{-1}$.

shown in Fig. 4, n and Ψ_1 are varied, while the other model parameters are held constant. If the kinetic chains are long with a high fraction of PVA molecules crosslinking it to the network (e.g. $n = 10,000$, Fig. 4A, curve A), mass loss happens over an extended time with a very distinct erosion profile. In this curve, there is an initial period where little or no erosion of the network occurs, although some of the crosslinks are being degraded. After enough of the crosslinks have degraded, the PVA chains begin to be released and a region of sustained mass loss results. At much later times, a plateau region is observed when the kinetic chains start to be slowly released. Once the kinetic chains start to be released, the network eventually reaches the reverse gelation point, at a time that is related to the number of crosslinks in the kinetic chains. When the number of PVA molecules connected to the kinetic chain decreases from 10,000 (Fig. 4, curve A) to 50 (Fig. 4, curve B), and then to 10 (Fig. 4, curve C), the reverse gelation point shifts dramatically from ~80 to ~38 to ~22 days. When the kinetic chains are less connected into the network, they release sooner; no plateau region is observed; and the overall time for complete degradation decreases. Decreasing the number of PVA molecules crosslinking the kinetic chains not only results in shortening the time for degradation, but also results in decreasing the percent mass loss that occurs before reverse gelation. For these three curves (i.e. $n = 10,000$, 50, and 10), the percent mass loss at reverse gelation was 83, 44, and 12%, respectively.

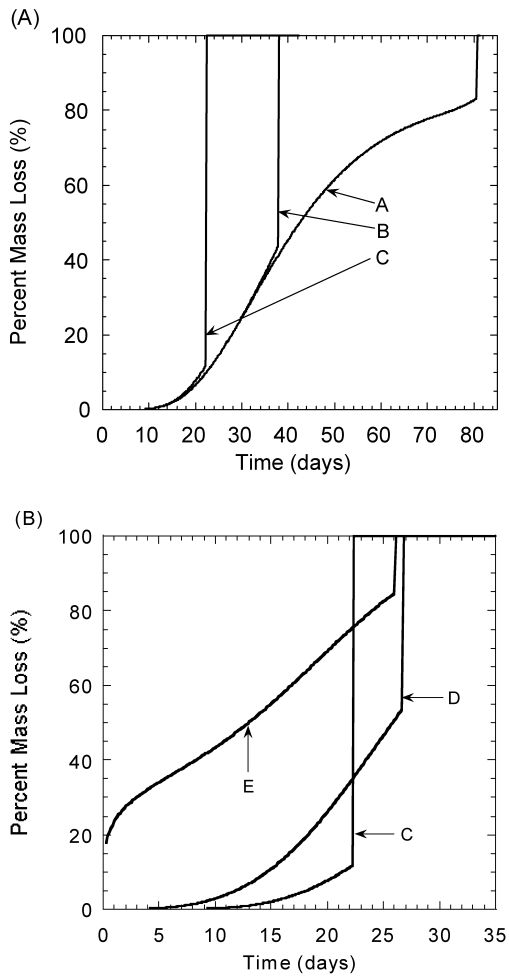

Fig. 4. Theoretical predictions of percent mass loss as a function of degradation time. For curves A, B, and C the number of crosslinking molecules in the kinetic chain, n, is varied from 10,000 to 50 to 10, and no cyclization is present. For curves D and E, $n = 10$, and the cyclization parameter, Ψ_1, is increased to 0.50 and 0.60, respectively. Other model parameters are: $m = 8$, $W_{x1} = 0.847$, and $k' = 4.5 \times 10^{-5}$ min^{-1}.

To further tailor the shape of the mass loss profile, variations in the extent of cyclization were also investigated. For example, if we look at just one of the previous curves ($n = 10$, Fig. 4A and B, curve C), and now add in cyclization, the time for degradation, the percent mass loss at reverse gelation, and the general shape of the curve are all affected. If Ψ_1 is set to 0.5 (Fig. 4B, curve D), the time for degradation is extended from 22 to 27 days; the percent mass loss at reverse gelation is increased from 12 to 60%; and the rate of mass loss is higher at equal time points. It is important to note here that when Ψ_1 is 0.0, the number of PVA molecules connected to the kinetic chain and the kinetic chain length are the same. However, by our definition of n, the kinetic chain length is longer when cyclization is present to keep the number of connections of the kinetic chains to the network constant (i.e. more functional groups must react into the kinetic chain to get the same number of crosslinks). This variation in the kinetic chain length not only leads to higher mass loss at the point of reverse gelation, but also leads to longer degradation times as there are more ester groups to be degraded per chain, even though the number of crosslinks is the same. Additionally, once a significant percent of cyclization is set, increasing Ψ_1 only results in small changes in the kinetic chain length; however, changing Ψ_1 from 0.50 to 0.60 (i.e. corresponding to an overall percent cyclization of 85.8 and 90.5%, respectively) results in a significant change in the mass loss profiles. When $\Psi_1 = 0.60$ (Fig. 4B, curve E), an immediate burst effect (20% mass loss) is noted, which means that some of the PVA chains have reacted completely upon themselves (i.e. formed cycles) and not with any other macromers in the system, and therefore, are not attached to the network. After the release of this initial, soluble fraction, the mass loss curve then follows a steady increase, similar to the other curves, and reaches a high percent mass loss (85%) before reverse gelation. From Fig. 4 parts A and B, one notes that a wide range of mass loss profiles can be achieved by careful selection of the macromer structure and/or polymerization conditions, and the ability to tailor the erosion profile can be beneficial for many biomaterial applications. For example, in cell encapsulation materials for tissue engineering, an initial burst of mass loss might be desired to allow for initial extracellular matrix secretion and deposition, followed by a slower mass loss as the tissue remodels with time. Alternatively, in other applications, such as in post-surgical adhesion prevention, a significant delay in mass loss may be advantageous to prevent the

in-growth of tissue, followed by relatively rapid polymer erosion after a predetermined period of time.

With a better theoretical understanding of the influence of various structural parameters on the overall mass loss profiles, validation of the model predictions was attempted by comparing model results to an experimental degradable hydrogel system synthesized from multi-functional, PVA macromers. To compare the model predictions to experimental data, the volumetric swelling ratio, compressive modulus, and the percent mass loss as function of degradation time were measured experimentally. Both, the volumetric swelling ratio and the compressive modulus were used to measure the hydrolysis rate constant, k'. The Flory–Rehner equation relates the volumetric swelling ratio to the network crosslinking density ($Q \propto n_{xl}^{-3/5}$ for highly swollen gels) [28], and then through the psuedo first-order kinetics of hydrolysis, temporal changes in the crosslinking density were related to k'. Finally, one obtains:

$$Q \sim e^{3/5k't} \tag{8}$$

The typical dynamic swelling behavior for a network made from a 16,000 g/mol macromer with an average of five crosslinkable functionalities per PVA chain is shown in Fig. 5A. As predicted by Eq. (8), the volumetric swelling ratio increased as a function of degradation time, due to the hydrolysis of the crosslinks. As the crosslinks are degraded, the crosslinking density decreases, and a more loosely crosslinked network swells to a greater degree. An exponential function was fit to the experimental data, which provides an estimate of the degradation rate constant for this system ($k' = 4.0 \times 10^{-5}$ min^{-1}).

The compressive modulus, K, was also used to determine the hydrolysis rate constant, k', as well as verify the k' calculated from the volumetric swelling ratio data. The rubber elasticity theory for swollen networks was used to relate the compressive modulus to the average molecular weight between crosslinks and the volumetric swelling ratio ($K \propto Qn_{xl}^{9/5}$) [31]. Since $Q \propto n_{xl}^{-3/5}$ and $n_{xl} \propto e^{-k't}$, temporal changes in the compressive modulus are given by:

$$K \sim e^{-6/5k't} \tag{9}$$

A typical plot of the compressive modulus as a function of degradation time is shown in Fig. 5B. As predicted by Eq. 9, the compressive modulus decreased as a function of degradation time due to the hydrolysis of the crosslinks. As the crosslinks are degraded, the crosslinking density decreases, and the network modulus decreases. An exponential function was fit to the experimental data, which provides the degradation rate constant ($k' = 4.0 \times 10^{-5}$ min^{-1}), which agrees with the estimate from the volumetric swelling data.

Once the hydrolysis rate constant was determined, the experimentally measured percent mass loss for the hydrogel network was compared to theoretical predictions. This comparison is shown in Fig. 6 and corresponds to the system

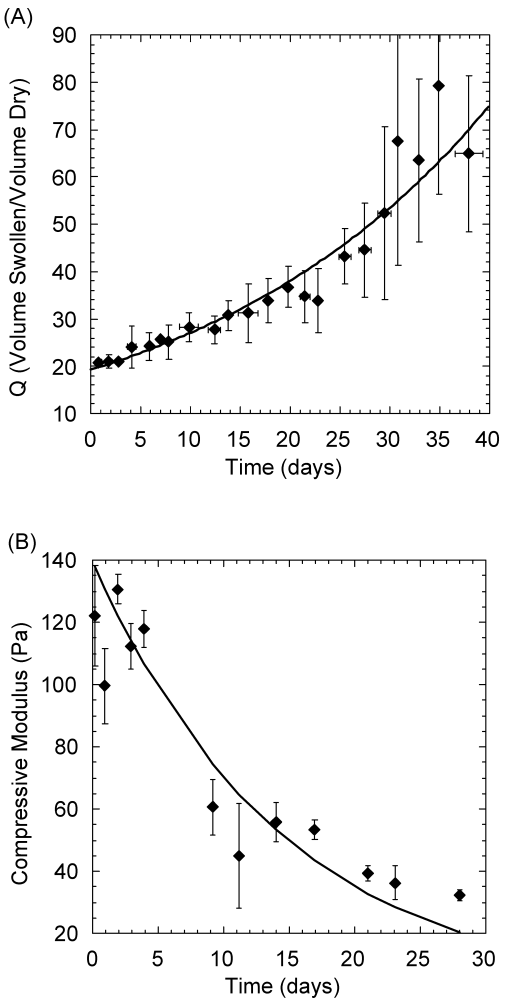

Fig. 5. Experimentally measured volumetric swelling ratio (A) and compressive modulus (B) as a function of degradation time. The network was formed from a 20 wt% solution of the 16,000 g/mol PVA macromer with an average of five crosslinkable functionalities per PVA chain. The data points are experimental data and the lines are exponential fits of the data.

whose volumetric swelling data and compressive modulus data are presented in Fig. 5 (i.e. 16,000 g/mol PVA with an average of five crosslinkable functionalities per PVA chain; model inputs are: $m = 5, W_{xl} = 0.899$, and $k' = 4.0 \times 10^{-5}$ min^{-1}). The other two parameters, n and Ψ_1, were variable parameters fit to the data. Specifically, n is strongly related to the point where reverse gelation occurs and was fit based on the data in this region ($n = 40$). Ψ_1 influences the shape of the curve and was estimated to be 0.5, based on the best fit of the data by minimizing the square of the deviation of the predicted versus experimentally measured data points. From Fig. 6, the model predictions are shown to follow the trends in the experimental data fairly well. All three regions of mass loss are easily seen in both the theoretical and experimental curves. The deviation that can be seen at the early times may be a result of a small fraction of chains that have a fewer number of vinyl groups attached.

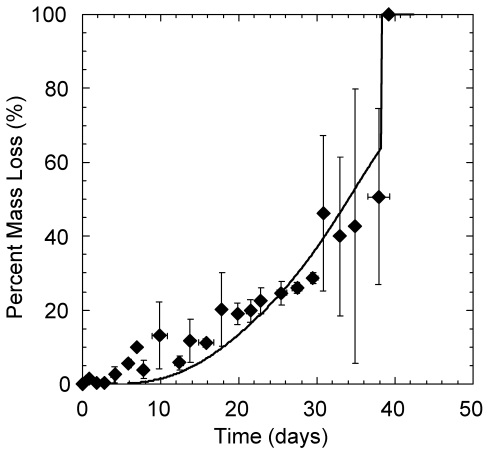

Fig. 6. Experimentally measured mass loss as a function of degradation time. The data points are experimental results, and the continuous line is the model predictions for a network formed from a 20 wt% solution of the 16,000 g/mol PVA with an average of five crosslinkable functionalities per PVA chain. Model parameters: $m = 5$, $n = 40$, $W_{xl} = 0.899$, $\Psi_1 = 0.5$, $k' = 4.0 \times 10^{-5}$ min^{-1}.

To demonstrate further the validity of the model and the ability to tailor mass erosion with these materials, the same approach was applied to a variety of networks formed from these macromers, and the model parameters were rationally changed to fit the experimental system. For instance, the initial crosslinking density of the hydrogel was varied by changing the molecular weight of the PVA backbone from 14,000 to 31,000 g/mol, while keeping the acrylate substitution similar (i.e. 3 vs. 2 acrylates per PVA chain, respectively). In this case, the initial crosslinking density changes from 0.27 mol/l for the 14,000 g/mol PVA to 0.08 mol/l for the 31,000 g/mol PVA. The volumetric swelling ratio and compressive modulus for networks formed from these two different PVA macromers are shown in Fig. 7A and B. From these graphs, one observes that both systems are highly swollen ($Q > 10$) and exhibit the expected exponential trends in Q and K with time. The volumetric swelling ratio increases exponentially, while the compressive modulus decreases exponentially for both systems. In addition, the more highly crosslinked system also exhibits a lower swelling ratio and a higher modulus at all time points (e.g. $Q_i = 18$, $K_i = 90$ Pa for the 14,000 g/mol PVA macromer and $Q_i = 34$, $K_i = 60$ Pa for the 31,000 g/mol PVA macromer). The hydrolysis rate constant was calculated from both the swelling and compressive modulus plots for each network ($k'_{14K} = 2.9 \times 10^{-5}$ min^{-1} for the 14,000 g/mol PVA macromer, and $k'_{31K} = 1.50 \times 10^{-5}$ min^{-1} for the 31,000 g/mol PVA macromer).

Once the hydrolysis rate constants were obtained, the model was used to predict the mass loss profiles of the networks (Fig. 8). For these networks, the number of functional groups (m), k', and the weight fraction of PVA chains ($W_{xl} = 0.928$ and 0.977 for the 14,000 and 31,000 g/mol PVA macromers, respectively) were all independently

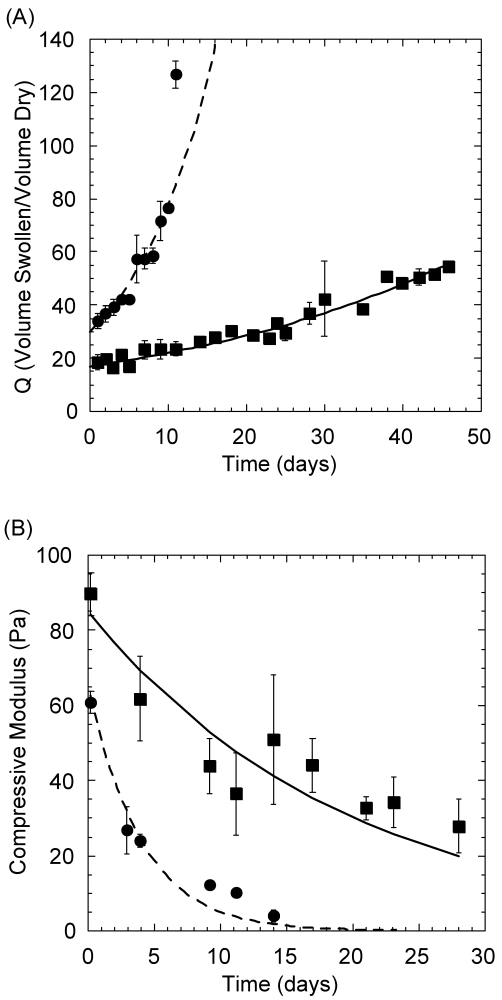

Fig. 7. Volumetric swelling ratio (A) and compressive modulus (B) as a function of degradation time. 20 wt% solutions of 31,000 g/mol with an average of two crosslinkable functionalities per PVA chain[32] (●, broken line) and 14,000 g/mol macromers with an average of three crosslinkable functionalities per PVA chain (■, continuous line) were used to synthesize the polymer networks. The points are experimental data and the lines are exponential fits.

determined. The remaining two model parameters, the number of crosslinking molecules in the kinetic chain and the percent cyclization, are dependent on the type of network that is formed during the polymerization. For the examples here, the reaction conditions were identical and these two parameters were kept constant at 50 crosslinking molecules per chain (n) and Ψ_1 equal to 0.5. By keeping these two parameters constant between these two networks, the importance of the hydrolysis kinetics, k', is illustrated. However, it is recognized that variations may exist in the kinetic chains and cyclization, since the polymerization is not taking place in the exact same environment (i.e. the initial macromer structure is different). Slight variations may exist in n and Ψ_1 and could be readily included in the model predictions; however, the current model predictions capture essential features of the mass loss profiles.

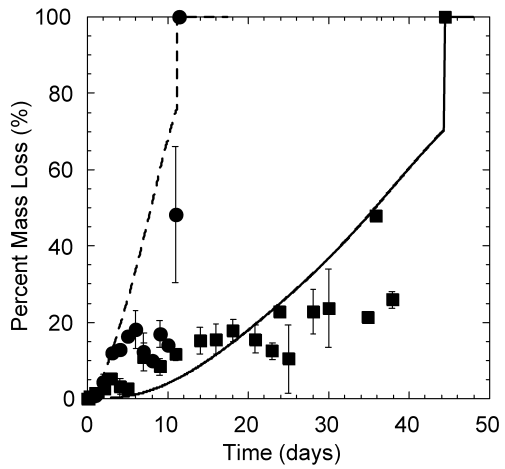

Fig. 8. Percent mass loss as a function of degradation time. 20 wt% solutions of 31,000 g/mol with an average of two crosslinkable functionalities per PVA chain [32] (●, broken line) and 14,000 g/mol macromers with an average of three crosslinkable functionalities per PVA chain (■, continuous line) were used to make the polymer networks. The points are experimental data and the lines are model predictions ($m_{14K} = 3$, $m_{31K} = 2$, $n = 50$, $\Psi_1 = 0.5$, $k'_{14K} = 2.9 \times 10^{-5}$ min^{-1}, and $k'_{31K} = 1.50 \times 10^{-4}$ min^{-1}).

4. Conclusions

Experimental and theoretical approaches were used to understand and better characterize the degradation behavior of networks formed from multi-functional macromers. A typical experimental mass loss profile was shown to illustrate the three main regions of erosion: an initial delay, sustained mass loss and reverse gelation. A statistical-kinetic model with five parameters was used to fit and predict the experimental mass loss profiles from those gels. The effect of changing the connectivity of the kinetic chains versus the PVA chains on the percent mass loss at reverse gelation was characterized. As either type of chain becomes more connected into the network, the mass loss before reverse gelation increases. In addition, the cyclization parameter and the number of crosslinking molecules connected to the kinetic chains were systematically varied, and produced a wide range of mass loss profiles. The general shape of the mass loss curve was varied, as well as the overall time needed for complete degradation (i.e. ranged from ~10 to 80 days).

After investigating what model parameters could be manipulated to produce mass loss profiles of several desired shapes, experimental results were compared to the model predictions. Volumetric swelling and compressive modulus data were obtained as a function of degradation time, and from this data, a hydrolysis rate constant was obtained and verified. Once the hydrolysis rate constant was known, the resulting mass loss predictions were compared to experimental data. A comparison between networks formed from different crosslinking densities was made, and the model captured many of the key portions of the mass loss profile for all of the experimental systems.

Acknowledgements

The authors would like to thank the National Science Foundation (BES-934236) and the National Institutes of Health (DE 12998) for support of this work through grants, BioCure Inc. for support of this work through an internship for P.M., as well as the Department of Education (GAANN) and the Colorado Institute for Research in Biotechnology for fellowships to P.M. The technical assistance of Jason Bara in obtaining portions of the experimental data is acknowledged and appreciated.

References

[1] van Dijk-Wolthuis WNE, Franssen O, Talsma H, van Steenbergen MJ, Kettenes-van den Bosch JJ, Hennink WE. Macromolecules 1995; 28:6317–22.
[2] Franssen O, van Ooijen RD, de Boer D, Maes RAA, Herron JN, Hennink WE. Macromolecules 1997;30:7408–13.
[3] Franssen O, Vos OP, Hennink WE. J Controlled Release 1997;3: 237–45.
[4] Hennink WE, Talsma H, Borchert JCH, De Smedt SC, Demeester J. J Controlled Release 1996;39:47–55.
[5] De Smedt SC, Meyvis TKL, Demeester J, Van Oostveldt P, Blonk JCG, Hennink WE. Macromolecules 1997;30(17):4863–70.
[6] Kumar GS, Kalpagam V, Nandi US. J Appl Polym Sci 1981;26: 3633–41.
[7] Nagabhushanam T, Santappa M. J Polym Sci 1976;14:507–10.
[8] van Dijk-Wolthuis WNE, Hoogeboom JAM, van Steenbergen MJ, Tsang SKY, Hennink WE. Macromolecules 1997;30(16):4639–45.
[9] Franssen O, Stenekes RJH, Hennink WE. J Controlled Release 1999; 59(2):219–28.
[10] Hennink WE, Franssen O, van Dijk-Wolthuis WNE, Talsma H. J Controlled Release 1997;48(2–3):107–14.
[11] Meyvis TKL, De Smedt SC, Demeester J, Hennink WE. Macromolecules 2000;33(13):4717–25.
[12] Franssen O, Vandervennet L, Roders P, Hennink WE. J Controlled Release 1999;60(2–3):211–21.
[13] Ulbrich K, Strohalm J, Kopecek J. Biomaterials 1982;3:150–4.
[14] Subr V, Duncan R, Kopecek J. J Biomater Sci-Polym Ed 1990;1(4): 261–78.
[15] Suggs LJ, Payne RG, Yaszemski MJ, Alemany LB, Mikos AG. Macromolecules 1997;30:4318–23.
[16] Peter SJ, Kim P, Yasko AW, Yaszemski MJ, Mikos AG. J Biomed Mater Res 1999;44:314–21.
[17] Metters AT, Bowman CN, Anseth KS. J Phys Chem B 2000;104(30): 7043–9.
[18] Metters AT, Anseth KS, Bowman CN. J Phys Chem B 2001;105(34): 8069–76.
[19] Metters AT, Bowman CN, Anseth KS. AIChE J 2001;47(6):1432–7.
[20] Mason MN, Metters AT, Bowman CN, Anseth KS. Macromolecules 2001;34(13):4630–5.
[21] Martens P, Metters AT, Anseth KS, Bowman CN. J Phys Chem B 2001;105(22):5131–8.
[22] Hirt T, Holland T, Francis V, Chaouk H. World Intellectual Property Organization. USA: BioCure, Inc; 2001.
[23] Martens P, Holland T, Anseth KS. Polymer 2002;43:6093–100.
[24] Martens P, Anseth KS. Polymer 2000;41(21):7715–22.
[25] Miyazaki K, Horibe T. J Biomed Mater Res 1988;22(11):1011–22.
[26] Bryant SJ, Nuttelman CR, Anseth KS. J Biomater Sci-Polym Ed 2000; 11(5):439–57.
[27] Martens P. Chemical engineering. Boulder: University of Colorado; 2002.

[28] Flory PJ. Principles of polymer chemistry. Ithaca, New York: Cornell University Press; 1953.
[29] Elliott JE, Bowman CN. Macromolecules 1999;32(25):8621–9.
[30] Martens P, Bryant S, Anseth KS. Biomacromolecules 2003;4(2): 282–92.
[31] Anseth KS, Bowman CN, Brannon-Peppas L. Biomaterials 1996;17: 1647–57.
[32] The original data reported in Polymer 2002;43,6093–100 reported the number of vinyl groups as 7; however, further purification and a more accurate analysis showed that the number of vinyl groups was 2.